

From Word2Vec to Transformers: Text-Derived Composition Embeddings for Filtering Combinatorial Electrocatalysts

Lei Zhang^{a)} and Markus Stricker

*Interdisciplinary Centre for Advanced Materials Simulation,
Ruhr University Bochum, Universitätsstraße 150, 44801 Bochum,
Germany*

(Dated: 11 March 2026)

Compositionally complex solid solution electrocatalysts span vast composition spaces, and even one materials system can contain more candidate compositions than can be measured exhaustively. Here we evaluate a label-free screening strategy that represents each composition using embeddings derived from scientific texts and prioritizes candidates based on similarity to two property concepts. We compare a corpus-trained Word2Vec baseline with transformer-based embeddings, where compositions are encoded either by linear element-wise mixing or by short composition prompts. Similarities to ‘concept directions’, the terms conductivity and dielectric, define a 2-dimensional descriptor space, and a symmetric Pareto-front selection is used to filter candidate subsets without using electrochemical labels. Performance is assessed on 15 materials libraries including noble metal alloys and multicomponent oxides. In this setting, the lightweight Word2Vec baseline, which uses a simple linear combination of element embeddings, often achieves the highest number of reductions of possible candidate compositions while staying close to the best measured performance.

Keywords: word embeddings, transformers, text mining, composition representation

I. INTRODUCTION

Compositionally complex solid solution materials, including high-entropy alloys and multicomponent oxides, provide a large compositional design space for electrocatalyst discovery because small changes in elemental identity and ratio can shift electronic structure, surface chemistry, and charge transport¹. Combinatorial synthesis and high-throughput electrochemical measurements enable comparatively rapid exploration of this space², but even a single library can contain hundreds to thousands of distinct compositions prepared under specific processing conditions^{3,4}. As library size and chemical diversity increase, deciding which compositions merit further measurement or deeper characterisation becomes a central practical step in experimental workflows.

Screening strategies in this setting must balance two needs that pull in different directions: reducing the number of candidates enough to save experimental effort while still keeping at least one near-top performer for a given material system and operating condition. Supervised learning can be effective when labelled data are abundant, consistent, and comparable across libraries^{5,6}, yet in practice measurements are often sparse, material system-specific, and influenced by preparation details. This makes it attractive to consider approaches that can operate with weak or no labels and that reuse information already present in the scientific record.

Scientific texts provide a compact representation of community knowledge linking composition to property language that is not a direct proxy for electrochemical response but often

^{a)}Electronic mail: lei.zhang-w2i@rub.de

reflects underlying physical constraints and correlations^{7,8}. The materials and electrocatalysis literature repeatedly connects composition to descriptors such as electrical conductivity, dielectric behavior, oxidation tendencies, and other recurring concepts^{9–11}. If compositions can be embedded into a latent space derived from text, then similarity to selected concept directions can define a low-dimensional descriptor space for ranking and filtering candidates in a way that is transferable across different libraries¹².

At the same time, a text-guided filter depends sensitively on how a multicomponent composition is represented within the embedding model^{13,14}. One option is to represent a composition as a concentration-weighted mixture of element embeddings, which is computationally straightforward and naturally supports fast screening, but it assumes linearity and independence across elements¹⁵. Another option is to embed a formatted full-composition prompt as a single piece of text, allowing the encoder to represent stoichiometric ratios and multi-element motifs more directly, but introducing choices about prompt design and model behavior¹⁶. Different embedding backbones further impose different inductive biases: lightweight distributional models trained on a focused corpus emphasise co-occurrence structure¹⁷, while transformer encoders may inject broader contextual associations learned during pretraining¹⁸. These modelling decisions shape both how aggressively candidate compositions in a given materials space, e.g. a materials library, can be reduced and how reliable high-performing compositions remain in the retained subset that comprises ‘the prediction’.

In this work, we construct text-derived composition embeddings using Word2Vec^{19–21}, MatSciBERT²², and Qwen²³ in both element-wise and full-composition prompt forms, project each composition onto concept directions related to electrical conductivity and dielectric behavior, and apply a dual Pareto-front filter to select candidates. We evaluate the resulting trade-offs between best-current retention and candidate reduction across 15 combinatorial libraries spanning the hydrogen evolution reaction (HER), oxygen reduction reaction (ORR), and oxygen evolution reaction (OER).

II. METHODS

A. Corpus collection (Word2Vec baseline)

For the Word2Vec baseline, scientific abstracts related to electrocatalysis, high-entropy alloys and complex oxides are collected using the `PaperCollector` module of the `MatNexus` framework²⁴. Abstracts are sourced from Scopus and arXiv, restricted to open-access publications available up to the year 2024. Only English-language abstracts are included. Metadata and full-text abstracts are automatically retrieved and stored in structured CSV format. This corpus is used exclusively to train the Word2Vec model; the transformer-based models (MatSciBERT and Qwen variants) are used in inference-only mode without additional training or fine-tuning on this corpus.

B. Text preprocessing (Word2Vec baseline)

Raw abstracts are processed using the `TextProcessor` module in `MatNexus`. Preprocessing includes removal of licensing statements and publisher-specific fragments (for example, “©” strings or publisher boilerplate), standard stopword filtering and sentence segmentation. Chemical element symbols and formulas are explicitly preserved to maintain their semantic relevance for materials-related embeddings. The cleaned, tokenised abstracts form the input for training the Word2Vec model. Transformer-based embeddings operate directly as pre-trained encoders and do not require this corpus-level preprocessing.

C. Construction of text-derived composition embeddings

Each composition in the experimental materials libraries is represented as a vector in a latent “text space”, and all downstream analysis (similarity to concepts and Pareto filtering) is performed on these vectors. The models differ only in how this composition embedding is constructed; the similarity and Pareto procedures are identical across all methods.

1. Word2Vec baseline (W2V)

As a lightweight baseline, we train word embeddings using the skip-gram architecture implemented in the `VecGenerator` module of `MatNexus`, based on the Word2Vec model^{19–21}. Compared with TF-IDF or large transformer models, Word2Vec provides compact, dense vector representations at comparatively low computational cost, making it suitable for focused scientific corpora²⁵. Training is performed with 200-dimensional vectors, a window size of 5, hierarchical softmax and a minimum word frequency of 1. All available CPU threads are used for parallelisation.

Element symbols (for example, “Ag”, “Pd”, “Pt”) are treated as ordinary tokens in the corpus. For a given binary or multicomponent composition c , we first extract the normalised atomic fractions of all present elements from the materials library (for example, $\text{Ag}_{0.5}\text{Pd}_{0.5}$). The corresponding composition vector $\mathbf{v}_{\text{W2V}}(c)$ is computed as a concentration-weighted linear combination of the element embeddings,

$$\mathbf{v}_{\text{W2V}}(c) = \sum_i x_i \mathbf{w}_i,$$

where x_i is the atomic fraction of element i and \mathbf{w}_i is its Word2Vec embedding. The resulting vector is ℓ_2 -normalised prior to similarity calculation. An example of the composition embeddings distribution is shown in Fig. ?? a).

2. Element-wise transformer embeddings (MatSciBERT and Qwen)

To probe the benefit of contextual transformer embeddings while retaining the simple linear-combination scheme, we construct element-wise material vectors using two models:

- MatSciBERT²²: a domain-specific transformer model applied to short element sentences.
- Qwen²³: a Qwen-based embedding model accessed via the Blablador service²⁶, using the same element-sentence prompts.

For each chemical element E present in the periodic table, we construct a short natural-language prompt of the form “**E** is a **chemical element**.” and encode this sentence once with the corresponding embedding model. This yields an element embedding \mathbf{e}_E for each element (MatSciBERT and Qwen separately). Rows in the composition data of the experimental materials library tables contain element-wise atomic fractions; these are clipped to non-negative values and renormalised to sum to one for each composition.

For a given composition c , such as $\text{Ag}_{0.5}\text{Pd}_{0.5}$, the element-wise transformer vector is defined as the concentration-weighted sum of the element vectors,

$$\mathbf{v}_{\text{elem}}(c) = \sum_i x_i \mathbf{e}_{E_i},$$

followed by ℓ_2 normalisation. This procedure is analogous to the Word2Vec baseline but replaces the distributional word vectors with transformer-derived element embeddings. We refer to the resulting models as MatSciBERT and Qwen throughout the manuscript. Both transformer models are used strictly in inference mode; no additional fine-tuning is performed on our electrocatalysis corpus.

3. Composition-prompt transformer embeddings (MatSciBERT_Full and Qwen_Full)

In addition to the element-wise representations, we consider models that operate directly on a textual description of the full composition. For each composition, we construct a prompt of the form

material composition: Ag = 0.50, Pd = 0.50,

optionally augmented with simple process tags (for example, co-sputtering, annealing temperature) when available. This prompt encodes both the identity of the elements and their relative fractions as a single piece of text.

Two composition-prompt models are evaluated:

- **MatSciBERT_Full:** the MatSciBERT model applied directly to the composition prompt.
- **Qwen_Full:** the Qwen-based Blablador embedding model applied to the same composition prompt.

For each row in the library table, the corresponding composition prompt is tokenized and passed through the embedding model. We use mean pooling over the last hidden layer to obtain a single fixed-length vector per composition (MatSciBERT_Full), or the embedding returned by the Blablador endpoint (Qwen_Full). All composition vectors are ℓ_2 -normalised. In contrast to the element-wise schemes, these models are free to encode higher-order interactions between elements and their stoichiometric ratios directly in text space.

D. Concept similarity scores

All models share the same concept layer and downstream similarity calculation. We select two simple, physically motivated descriptors that frequently appear in discussions of electrocatalytic materials and related thin films: **conductivity** and **dielectric**²⁷.

For the Word2Vec model, we use the individual tokens “conductivity” and “dielectric” and extract their corresponding word embeddings. An example of the resulting similarity-score distribution in the two-concept space is shown in Fig. ?? b). For the transformer-based models, we encode short natural-language phrases, such as “**conductivity material property**” and “**dielectric material property**”, to obtain concept vectors. In all cases, the concept vectors are ℓ_2 -normalised.

Given a normalised composition vector $\mathbf{v}(c)$ (from W2V, MatSciBERT, Qwen, MatSciBERT_Full or Qwen_Full) and a normalised concept vector \mathbf{v}_k (for $k \in \{\text{conductivity, dielectric}\}$), we compute cosine similarity,

$$S_k = \mathbf{v}(c) \cdot \mathbf{v}_k.$$

Thus, each composition is mapped to a point $(S_{\text{dielectric}}, S_{\text{conductivity}})$ in a two-dimensional descriptor space derived purely from text.

E. Pareto-front multi-objective filtering

Multi-objective optimization is performed via Pareto front analysis in the two-dimensional descriptor space spanned by similarity to the dielectric- and conductivity-related concepts. A composition is considered Pareto-optimal if no other composition achieves equal or better performance across all objectives²⁸.

Because the two descriptors correspond to complementary electronic regimes that can both be desirable in electrocatalysts, we do not assign one concept as universally favourable. Instead, we construct two Pareto fronts with opposite objective directions:

1. Maximize similarity to **conductivity** while simultaneously minimizing similarity to **dielectric**;
2. Maximize similarity to **dielectric** while simultaneously minimizing similarity to **conductivity**.

For each embedding model and each material system, non-dominated compositions are identified separately in the corresponding objective space. The final candidate set used for experimental comparison is the union of the two fronts, ensuring a symmetric treatment of the two concepts. The same dual-front construction is applied uniformly to all embedding models (W2V, MatSciBERT, Qwen, MatSciBERT_Full and Qwen_Full) and to all alloy and oxide libraries considered in this study.

III. RESULTS

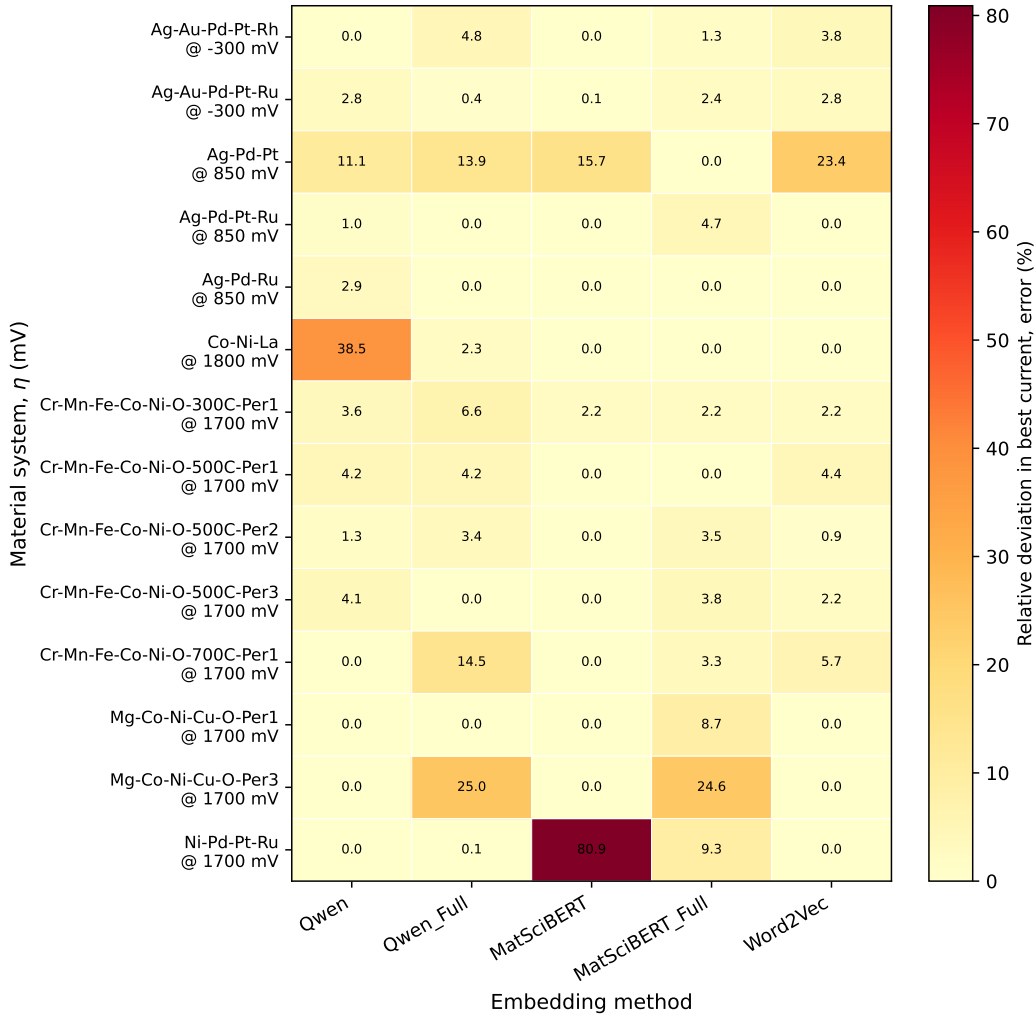


FIG. 1. Heatmap of the relative error in the current density of the best-performing composition between the Pareto-selected subset and the all compositions of the respective materials library. Colour indicates the percentage deviation, with lighter shades for smaller errors and darker shades for larger errors.

TABLE I. Performance of W2V, MatSciBERT, and Qwen across all material systems and overpotentials. Here, count/O and count/P denote the number of compositions in the original dataset and in the Pareto-selected subset, respectively; best/O and best/P are the best current densities in each set (mA cm^{-2}); error (%) is the relative deviation between best/P and best/O; and fraction (%) is the percentage of original candidates retained in the Pareto subset.

Material system	η (mV)	Method	count/O	count/P	best/O	best/P	error (%)	fraction (%)
Ag-Au-Pd-Pt-Rh	-300	MatSciBERT	327	154	-1.1	-1.1	0.0	47.1
		Qwen	327	93	-1.1	-1.1	0.0	28.4
		W2V	327	9	-1.1	-1.1	3.8	2.8
Ag-Au-Pd-Pt-Ru	-300	MatSciBERT	335	88	-1.5	-1.5	0.1	26.3
		Qwen	335	109	-1.5	-1.5	2.8	32.5
		W2V	335	20	-1.5	-1.5	2.8	6.0
Ag-Pd-Pt	850	MatSciBERT	341	45	-0.6	-0.5	15.7	13.2
		Qwen	341	71	-0.6	-0.5	11.1	20.8
		W2V	341	15	-0.6	-0.4	23.4	4.4
Ag-Pd-Pt-Ru	850	MatSciBERT	341	49	-0.4	-0.4	0.0	14.4
		Qwen	341	86	-0.4	-0.4	1.0	25.2
		W2V	341	13	-0.4	-0.4	0.0	3.8
Ag-Pd-Ru	850	MatSciBERT	342	50	-0.7	-0.7	0.0	14.6
		Qwen	342	63	-0.7	-0.7	2.9	18.4
		W2V	342	14	-0.7	-0.7	0.0	4.1
Co-Ni-La	1800	MatSciBERT	342	232	2.2	2.2	0.0	67.8
		Qwen	342	289	2.2	1.4	38.5	84.5
		W2V	342	66	2.2	2.2	0.0	19.3
Cr-Mn-Fe-Co-Ni-O-300C-Per1	1700	MatSciBERT	342	303	1.9	1.8	2.2	88.6
		Qwen	342	66	1.9	1.8	3.6	19.3
		W2V	342	90	1.9	1.8	2.2	26.3
Cr-Mn-Fe-Co-Ni-O-500C-Per1	1700	MatSciBERT	342	306	2.3	2.3	0.0	89.5
		Qwen	342	68	2.3	2.2	4.2	19.9
		W2V	342	81	2.3	2.2	4.4	23.7
Cr-Mn-Fe-Co-Ni-O-500C-Per2	1700	MatSciBERT	342	297	2.7	2.7	0.0	86.8
		Qwen	342	96	2.7	2.7	1.3	28.1
		W2V	342	71	2.7	2.7	0.9	20.8
Cr-Mn-Fe-Co-Ni-O-500C-Per3	1700	MatSciBERT	342	243	2.2	2.2	0.0	71.1
		Qwen	342	104	2.2	2.1	4.1	30.4
		W2V	342	135	2.2	2.1	2.2	39.5
Cr-Mn-Fe-Co-Ni-O-700C-Per1	1700	MatSciBERT	342	291	1.5	1.5	0.0	85.1
		Qwen	342	62	1.5	1.5	0.0	18.1
		W2V	342	81	1.5	1.4	5.7	23.7
Mg-Co-Ni-Cu-O-Per1	1700	MatSciBERT	342	47	4.9	4.9	0.0	13.7
		Qwen	342	51	4.9	4.9	0.0	14.9
		W2V	342	49	4.9	4.9	0.0	14.3
Mg-Co-Ni-Cu-O-Per3	1700	MatSciBERT	342	85	4.3	4.3	0.0	24.9
		Qwen	342	67	4.3	4.3	0.0	19.6
		W2V	342	97	4.3	4.3	0.0	28.4
Ni-Pd-Pt-Ru	1700	MatSciBERT	4026	465	6.9	1.3	80.9	11.5
		Qwen	4026	846	6.9	6.9	0.0	21.0
		W2V	4026	391	6.9	6.9	0.0	9.7

We evaluate five text-derived embedding models on 15 combinatorial materials libraries covering HER (Ag-Au-Pd-Pt-Ru, Ag-Au-Pd-Pt-Rh), ORR (Ag-Pd-Pt, Ag-Pd-Pt-Ru, Ag-Pd-Ru) and OER systems. The OER set includes one metallic library (Ni-Pd-Pt-Ru) and several complex oxides with different preparation conditions. For each (system, overpotential, method) triple we report two quantities: (i) the retained fraction f_{ret} (%), defined as the percentage of original candidates kept in the Pareto-selected subset; and (ii) the performance deviation *error* (%), defined as the relative deviation between the best current density in the Pareto subset (best/P) and the best current density in the original library

TABLE II. Performance of MatSciBERT_Full and Qwen_Full across all material systems and overpotentials. Here, count/O and count/P denote the number of compositions in the original dataset and in the Pareto-selected subset, respectively; best/O and best/P are the best current densities in each set (mA cm^{-2}); error (%) is the relative deviation between best/P and best/O; and fraction (%) is the percentage of original candidates retained in the Pareto subset.

Material system	η (mV)	Method	count/O	count/P	best/O	best/P	error (%)	fraction (%)
Ag-Au-Pd-Pt-Rh	-300	MatSciBERT_Full	327	37	-1.1	-1.1	1.3	11.3
		Qwen_Full	327	55	-1.1	-1.1	4.8	16.8
Ag-Au-Pd-Pt-Ru	-300	MatSciBERT_Full	335	41	-1.5	-1.5	2.4	12.2
		Qwen_Full	335	74	-1.5	-1.5	0.4	22.1
Ag-Pd-Pt	850	MatSciBERT_Full	341	46	-0.6	-0.6	0.0	13.5
		Qwen_Full	341	61	-0.6	-0.5	13.9	17.9
Ag-Pd-Pt-Ru	850	MatSciBERT_Full	341	50	-0.4	-0.3	4.7	14.7
		Qwen_Full	341	81	-0.4	-0.4	0.0	23.8
Ag-Pd-Ru	850	MatSciBERT_Full	342	60	-0.7	-0.7	0.0	17.5
		Qwen_Full	342	65	-0.7	-0.7	0.0	19.0
Co-Ni-La	1800	MatSciBERT_Full	342	50	2.2	2.2	0.0	14.6
		Qwen_Full	342	71	2.2	2.2	2.3	20.8
Cr-Mn-Fe-Co-Ni-O-300C-Per1	1700	MatSciBERT_Full	342	39	1.9	1.8	2.2	11.4
		Qwen_Full	342	51	1.9	1.7	6.6	14.9
Cr-Mn-Fe-Co-Ni-O-500C-Per1	1700	MatSciBERT_Full	342	38	2.3	2.3	0.0	11.1
		Qwen_Full	342	38	2.3	2.2	4.2	11.1
Cr-Mn-Fe-Co-Ni-O-500C-Per2	1700	MatSciBERT_Full	342	33	2.7	2.6	3.5	9.6
		Qwen_Full	342	46	2.7	2.6	3.4	13.5
Cr-Mn-Fe-Co-Ni-O-500C-Per3	1700	MatSciBERT_Full	342	52	2.2	2.1	3.8	15.2
		Qwen_Full	342	37	2.2	2.2	0.0	10.8
Cr-Mn-Fe-Co-Ni-O-700C-Per1	1700	MatSciBERT_Full	342	41	1.5	1.4	3.3	12.0
		Qwen_Full	342	40	1.5	1.3	14.5	11.7
Mg-Co-Ni-Cu-O-Per1	1700	MatSciBERT_Full	342	46	4.9	4.5	8.7	13.5
		Qwen_Full	342	41	4.9	4.9	0.0	12.0
Mg-Co-Ni-Cu-O-Per3	1700	MatSciBERT_Full	342	41	4.3	3.2	24.6	12.0
		Qwen_Full	342	47	4.3	3.2	25.0	13.7
Ni-Pd-Pt-Ru	1700	MatSciBERT_Full	4026	105	6.9	6.3	9.3	2.6
		Qwen_Full	4026	123	6.9	6.9	0.1	3.1

(best/O), as reported in Tables I and II. Thus, $error = 0$ indicates that the Pareto subset contains a composition that matches the original best performer (best/P = best/O) (Tables I and II, Figs. 1–3). Changes in the spread of compositions are summarised by the IQR metrics (Table ?? and Table ??), and a representative spatial example for the Ag-Pd-Pt ORR library is shown in Fig. ??.

A. Element-wise embeddings across reaction types

The element-wise models (W2V, MatSciBERT, Qwen) share the same linear combination of element vectors but differ in the underlying text encoder. Across all systems, the Pareto subsets produced by these methods retain between a few percent and almost the full library (Table I and Table ??, Figs. 1 and 2).

For the HER libraries (Ag-Au-Pd-Pt-Ru and Ag-Au-Pd-Pt-Rh), all three element-wise models keep the most negative current densities essentially unchanged: $error \leq 4\%$ for all methods, with several cases of $error = 0$ (Table I, Fig. 1). The retained fraction spans from $f_{ret} \sim 3\text{--}6\%$ for W2V, through $f_{ret} \sim 25\text{--}33\%$ for Qwen, up to $f_{ret} \sim 26\text{--}47\%$ for MatSciBERT (Table I, Fig. 2).

For the ORR libraries (Ag-Pd-Pt, Ag-Pd-Pt-Ru, Ag-Pd-Ru) the same pattern holds. The performance deviation remains below $error \sim 25\%$ for all element-wise models, and below $error \sim 12\%$ in most cases (Table I, Fig. 1). W2V selects $f_{ret} \sim 4\text{--}5\%$ of compositions,

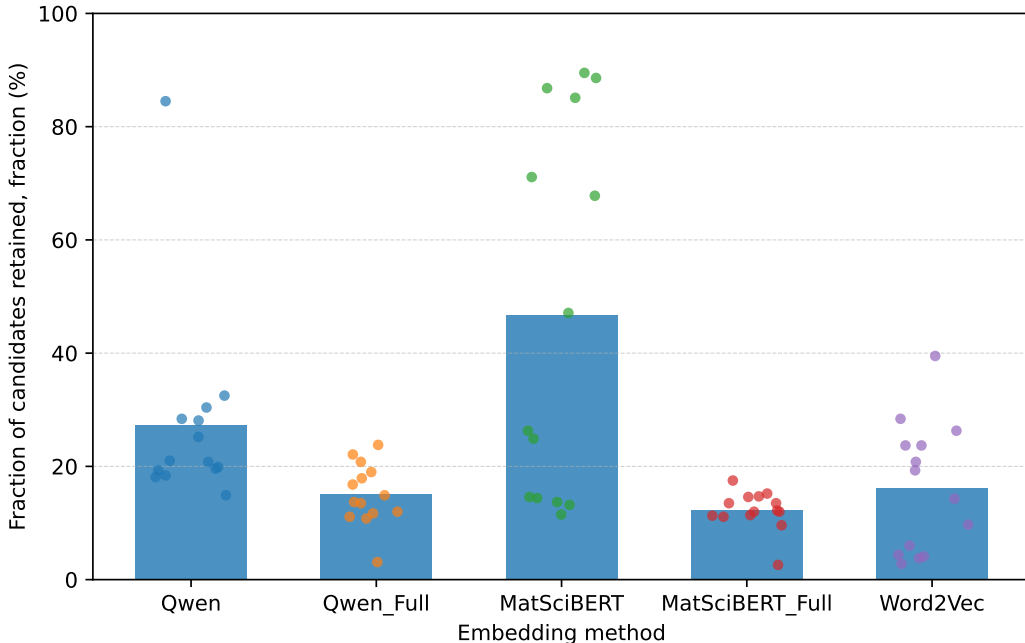


FIG. 2. Fraction of compositions retained in the Pareto-selected subset for each embedding method. Bars show the mean retained fraction across all material systems. The overlaid dots show the retained fraction for each individual material system; they are slightly shifted left/right only to prevent points from overlapping (the shift has no numerical meaning).

Qwen $f_{\text{ret}} \sim 18\text{--}25\%$, and MatSciBERT $f_{\text{ret}} \sim 13\text{--}15\%$ (Table I, Fig. 2). The IQR statistics for these noble-metal systems show mixed behavior: depending on the library and method, the Pareto subset can either narrow or broaden the composition distribution (Table ??).

For the oxide OER libraries, MatSciBERT tends to keep a large retained fraction (typically $f_{\text{ret}} = 70\text{--}90\%$ for the Cr-Mn-Fe-Co-Ni-O systems, and $f_{\text{ret}} = 14\text{--}25\%$ for Mg-Co-Ni-Cu-O), with *error* in the best current density mostly below 5% (Table I, Figs. 1 and 3). Qwen and W2V select smaller subsets ($f_{\text{ret}} \sim 18\text{--}40\%$ for Qwen and $f_{\text{ret}} \sim 20\text{--}40\%$ for W2V in the oxides), with *error* again generally below 5% (Table I). The metallic Ni-Pd-Pt-Ru library is an outlier: MatSciBERT retains $f_{\text{ret}} \sim 12\%$ of candidates but yields a large performance deviation (*error* $\sim 81\%$), whereas Qwen and W2V keep $f_{\text{ret}} \sim 21\%$ and $f_{\text{ret}} \sim 10\%$ of candidates, respectively, with *error* ≈ 0 (Table I, Fig. 1). The IQR results for the OER systems show that, for many element-wise runs, the Pareto subsets span a composition range similar to or broader than the original libraries (often negative IQR narrowing in Table ??).

B. Composition-prompt embeddings across reaction types

The composition-prompt models (MatSciBERT_Full, Qwen_Full) operate directly on formatted composition strings but follow the same Pareto selection procedure. Across all material systems, both full models typically retain $f_{\text{ret}} \sim 10\text{--}20\%$ of candidates, with Qwen_Full often keeping slightly more than MatSciBERT_Full (Table II and Table ??, Fig. 2).

In the HER libraries, both full models achieve small performance deviations, typically *error* $\lesssim 5\%$, and in several systems *error* = 0 (Table II, Fig. 1). The corresponding retained fractions lie at $f_{\text{ret}} \sim 11\text{--}22\%$, intermediate between W2V and the element-wise MatSciBERT approaches (Table I and Table II).

For the ORR systems, MatSciBERT_Full and Qwen_Full again preserve the top perfor-

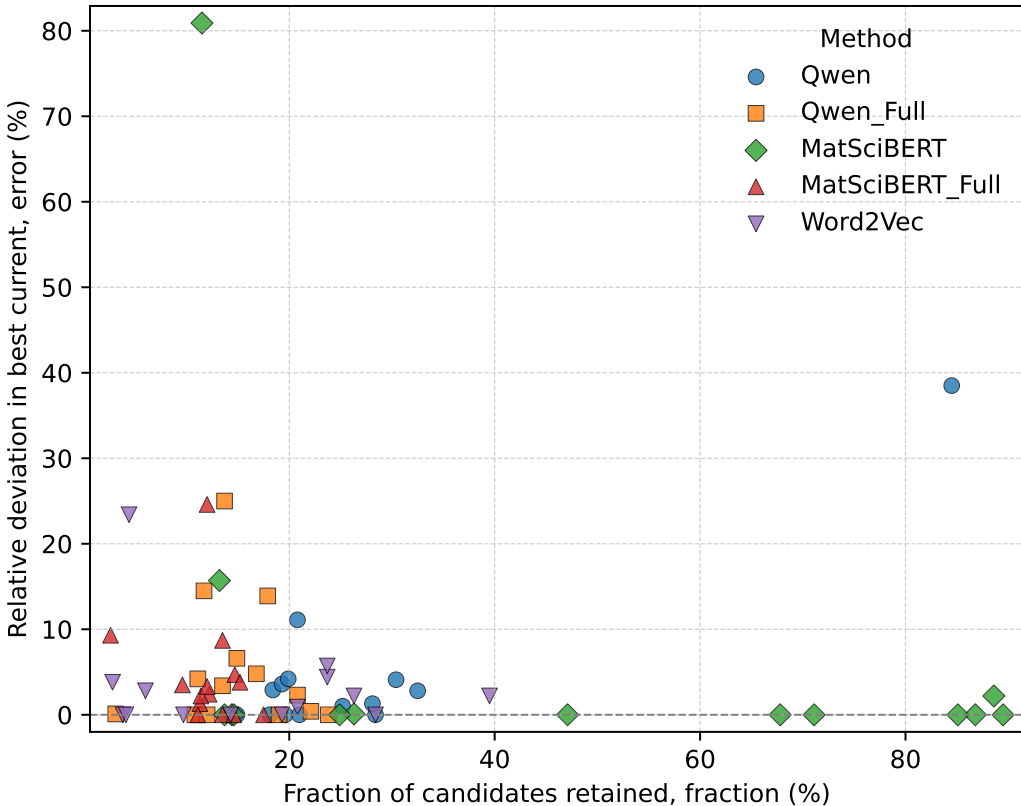


FIG. 3. Trade-off between the fraction of candidates retained and the relative error in the current density of the best-performing composition for all material systems and embedding methods.

mance with modest deviation ($error \sim 5\text{--}15\%$) while retaining $f_{ret} \sim 13\text{--}24\%$ of candidates (Table II). In the Ag-Pd-Pt library, MatSciBERT_Full yields $error = 0$ at $f_{ret} \sim 14\%$, whereas Qwen_Full shows $error \sim 14\%$ at $f_{ret} \sim 18\%$ (Table II, Fig. 3).

For the OER oxides, both composition-prompt models generally keep the deviation below $error \sim 10\%$, with a larger deviation ($error \sim 25\%$) in the Mg-Co-Ni-Cu-O-Per3 library for both MatSciBERT_Full and Qwen_Full (Table II). Retained fractions are $f_{ret} \sim 10\text{--}15\%$, comparable to HER and ORR. In the metallic Ni-Pd-Pt-Ru library, MatSciBERT_Full retains $f_{ret} \sim 3\%$ with $error \sim 9\%$, whereas Qwen_Full retains a similar fraction with essentially zero deviation ($error \approx 0$) (Table II, Figs. 1 and 3). The IQR shifts for the full models remain zero closer to zero than for the element-wise models, indicating moderate redistribution of compositions rather than systematic narrowing of composition ranges (Table ??).

C. Comparison between element-wise and full embeddings

Comparing models that share the same backbone allows the assessment of the impact of encoding the compositions as composition-weighted individual elements versus full composition strings. For the MatSciBERT pair, MatSciBERT usually retains a larger retained fraction than MatSciBERT_Full, especially in the OER oxides (e.g. $f_{ret} = 70\text{--}90\%$ vs. $f_{ret} \sim 10\text{--}15\%$ in the Cr-Mn-Fe-Co-Ni-O libraries; Table I and Table II, Fig. 2). The performance deviations are small for both, except for two cases: Ag-Pd-Pt (where MatSciBERT shows $error \sim 16\%$ vs. $error = 0$ for MatSciBERT_Full), and Ni-Pd-Pt-Ru ($error \sim 81\%$ for MatSciBERT vs. $error \sim 9\%$ for MatSciBERT_Full; Table I and Table II, Figs. 1 and 3).

For the Qwen pair, Qwen typically keeps a larger subset than Qwen_Full in the HER and ORR systems, whereas in many oxide OER systems their retained fractions are closer (Table I and Table II, Fig. 2). The performance deviations are mostly within $error \sim 5\%$ for both, with two larger values: Co-Ni-La ($error \sim 39\%$ for Qwen vs. $error \sim 2\%$ for Qwen_Full) and Mg-Co-Ni-Cu-O-Per3 ($error \approx 0$ for Qwen vs. $error \sim 25\%$ for Qwen_Full; Table I and Table II, Figs. 1 and 3).

Relative to the full models, W2V tends to select the smallest subsets across reaction types (typically $f_{ret} \sim 3\text{--}16\%$, with a few oxide systems around $f_{ret} \sim 25\text{--}30\%$; Table I and Table II, Fig. 2) while maintaining performance deviations within $error \sim 6\%$ for all libraries considered (Table I, Fig. 1). The IQR statistics show that W2V can either narrow or broaden the composition range depending on the system, with pronounced narrowing in Ni-Pd-Pt-Ru and several noble-metal libraries (Table ?? and Table ??).

D. Trade-off between candidate reduction and best-current deviation

The scatter plot of $error$ versus f_{ret} (Fig. 3) summarizes the trade-offs across all systems and methods. MatSciBERT points cluster at high retained fractions ($f_{ret} \gtrsim 40\%$) with performance deviations mostly below $error \sim 10\%$, apart from the Ni-Pd-Pt-Ru outlier. W2V points lie predominantly in the low-retention region ($f_{ret} \lesssim 20\%$) while remaining close to the horizontal axis, consistent with small deviations. Qwen, MatSciBERT_Full and Qwen_Full occupy intermediate positions in this plane, with retained fractions mostly in the $f_{ret} = 10\text{--}30\%$ range and deviations usually below $error \sim 10\%$ (Fig. 3). Within this global view, HER, ORR and OER systems are interleaved: for all three reaction types there exist configurations with small deviation at low, medium and high retained fractions.

E. Spatial sampling in a representative ORR library

The Ag-Pd-Pt ORR library illustrates how the Pareto subsets are distributed in real space. Panel (a) of Fig. ?? shows the full x - y layout of measured compositions colored by current density. Panels (b)-(f) display the corresponding Pareto-selected subsets for MatSciBERT, MatSciBERT_Full, Qwen, Qwen_Full and W2V, with the rest of the compositions shown in gray. In all cases, the Pareto subsets form sparse subsets of the full materials library rather than a tight cluster, with points chosen across a broad range of x and y . This qualitative pattern is consistent with the IQR results, which show modest narrowing or broadening of the composition distributions in the selected subsets rather than strong contraction to a small region (Table ?? and Table ??).

IV. DISCUSSION

We use text-derived composition embeddings, combined with a dual Pareto-front construction, as a filtering tool for combinatorial electrocatalyst materials libraries. Rather than aiming to predict current densities directly, our method ranks compositions in a two-dimensional descriptor space and selects those that are non-dominated with respect to two concept similarities.

The central question is whether such a filtering scheme based on text mining can discard a large fraction of candidates while still retaining at least one near-optimal composition in each library. Across HER, ORR and OER systems, our results show that this is often achievable: Pareto subsets are substantially smaller than the original materials libraries' composition range yet typically contain a composition whose current density is close to the best-measured value (Figs. 1-3, Table I and Table II).

A useful way to interpret these results is to separate the *shared selection pipeline* from the *embedding models* that feed into it. All methods map each composition to a vector in

a latent embedding space, then project this composition-representing vector onto two concept directions (‘conductivity’ and ‘dielectric’), and apply the same two-dimensional Pareto filtering. For the element-wise variants (W2V, MatSciBERT, Qwen), the composition vector itself is constructed as a linear combination of element embeddings weighted by atomic fraction. This downstream machinery is deliberately simple: linear mixing, normalization, two scalar similarities, and a Pareto filter. The transformer-based models differ only in how the element or composition vectors are obtained from text, not in how these vectors are used. The observation that such a minimal concept layer and linear mixing scheme can still identify subsets that preserve near-best-performing compositions suggests that, for the libraries studied here, ‘coarse’ text-derived representations capture fuzzy correlations that are mappable to electrocatalytic performance.

Within this common framework, comparing the three element-wise models highlights how the choice of encoder modulates the trade-off between filtering strength and robustness. In both HER and noble-metal ORR libraries, W2V, Qwen and MatSciBERT usually retain at least one composition with current density close to the best measured value, but the retained fractions differ systematically (Figs. 1-2, Table I). W2V tends to return the smallest subsets, Qwen occupies an intermediate regime, and MatSciBERT often retains the most candidate compositions, especially in the oxide OER libraries. This pattern is consistent with the idea that the three encoders impose broadly similar rankings on the compositions along the conductivity–dielectric axes, but differ in the detailed structure of that ordering. Small differences in relative similarity then translate into more or fewer points lying on the union of the two Pareto fronts.

The comparison between element-wise and composition-prompt models (MatSciBERT vs. MatSciBERT_Full, Qwen vs. Qwen_Full) shows how embedding the full composition string modifies this balance. The composition-prompt models are free to encode higher-order interactions between elements and stoichiometric ratios that are inaccessible to a purely linear mixture of independent element vectors. For some chemical systems, this extra flexibility appears beneficial w.r.t. candidate composition prediction: the full models can match or slightly improve the quality of the best-selected composition at similar or lower retained fractions, with the Ni-Pd-Pt-Ru OER system providing a clear example where MatSciBERT_Full avoids the large deviation seen for element-wise MatSciBERT (Table I and Table II). In other chemical systems, the full models behave similar to their element-wise counterparts, or show modestly larger deviations without a clear gain in filtering. These mixed outcomes indicate that composition prompts can help when the response depends on specific multi-element motifs or ratios that are well represented in text, but they are not uniformly advantageous across all reaction types and chemical systems.

Looking across reaction types, our method behaves most consistently in the HER and noble-metal ORR libraries. Here, the literature is rich in discussions of metallic conductivity, alloying trends and surface chemistry, and these topics are likely to be well captured in the electrocatalysis corpus used for training the embeddings. It is plausible that similarity to conductivity- and dielectric-related concepts aligns more directly with the underlying physics in these systems, so that even a coarse two-concept descriptor space is sufficient to highlight compositions that are experimentally active. The oxide OER libraries present a more demanding setting: activity is strongly influenced by oxidation state, local coordination, defects and transport through complex perovskite or spinel structures, which are only partially reflected in element names and simple composition-encoding strings. In this regime, element-wise MatSciBERT tends to keep a large fraction of the candidates and achieves small deviations, whereas W2V and Qwen more aggressively reduce the library at the cost of slightly larger errors (Table I, Fig. 3). The metallic Ni-Pd-Pt-Ru OER library highlights a different failure mode: element-wise MatSciBERT does not contain the best-performing composition, while W2V, Qwen and the full models avoid this bias. These observations support an interpretation in which the alignment between text-derived concept space and physical response is controlled jointly by the encoder, the corpus and the material class: good performance in one family of systems does not necessarily translate to similarly good behavior elsewhere.

The IQR analysis and the Ag-Pd-Pt spatial plots clarify how the Pareto filters the composition space of materials libraries. Across most model–system combinations, the elemental interquartile ranges in the Pareto subsets are comparable to those in the full libraries, and in several cases they are slightly broader (Table ?? and Table ??). The spatial distributions for Ag-Pd-Pt (Fig. ??) show that the selected points remain spread over the materials library: each model retains compositions along different arcs or clusters, but none collapses onto a single, narrow region. Gray points emphasize that most measured compositions are removed, yet the surviving candidates still cover multiple distinct parts of the materials library. This suggests that the method acts mainly as a point-wise filter that favors compositions with extreme values among the candidate compositions, rather than as a tool that sharply contracts the explored composition range. For exploratory screening, such behavior is attractive: it reduces the number of experiments while maintaining diversity in the retained compositions.

A recurring theme is the competitiveness of the simple W2V baseline. Despite exhibiting a comparatively small architecture and being trained on a small corpus and using only distributional statistics over element tokens, W2V often matches the transformer-based models in terms of retaining a near-best-performing composition at a given level of filtering, and in some libraries it offers a slightly better trade-off between error and retained fraction (Figs. 2 and 3). Because all models share the same linear mixing and Pareto pipeline, this points to the corpus statistics and the coarse choice of concept directions as the dominant factors for this task, with the additional representational capacity of transformers playing a secondary role. In practical terms, this supports the use of W2V-derived element embeddings as a reasonable, low-cost baseline for constructing text-derived descriptors of composition space, with transformer-based models providing an optional route in settings where their extra flexibility can be justified.

Our implementation nonetheless contains several deliberate simplifications that shape both its strengths and its limitations. The descriptor space is restricted to two concept directions and does not explicitly account for other factors known to influence electrocatalyst performance, such as stability, adsorption energy, or detailed structural information beyond the coarse processing tags included in the composition prompts. The evaluation focuses on the best current density at a single overpotential per system, so it does not probe how well the filter preserves other features of the electrochemical performance landscape. The embeddings are also influenced by how they are obtained. For the W2V baseline, the vectors depend directly on the electrocatalysis-focused corpus assembled in our work, as well as on the chosen training hyperparameters. In contrast, the transformer-based embeddings are taken from pre-trained MatSciBERT and Qwen models, whose underlying training data and objectives are defined externally and only partly documented. In all cases, we fixed the W2V corpus and the prompt templates used to generate element-wise or composition-prompt embeddings; the questions how a different corpora, possible pre-training mixtures or different prompt formulations might alter the behavior of the filtering process remains to be explored. Finally, the size of the Pareto subset is an emergent property of the objective space and cannot currently be tuned directly, and the method does not provide uncertainty estimates or formal guaranties on the retained error of the prediction.

Within these boundaries, our present results indicate that text-derived composition embeddings, combined with a simple concept layer and Pareto-front filtering, offer a practical way to reduce the candidate composition space of combinatorial materials libraries for electrochemical applications while retaining high-performing candidates for HER, ORR and OER. The fact that linear combinations of element embeddings from a Word2Vec model already perform well suggests that relatively modest text-derived representations can be sufficient for this kind of pre-screening, and that composition-prompt transformer embeddings provide an additional but not strictly necessary layer. In this sense, the approach does not replace detailed mechanistic modeling or supervised learning on experimental data but can complement them by providing an inexpensive, label-free filter that substantially narrows the experimental search space while retaining good-to-best-performing compositions across diverse material systems as high-probability search directions.

V. CONCLUSIONS

Text-derived composition embeddings combined with a two-concept similarity map and a dual Pareto-front filter provide a practical, label-free way to reduce combinatorial electrocatalyst libraries while retaining high-performing composition candidates across the hydrogen evolution reaction (HER), oxygen reduction reaction (ORR), and oxygen evolution reaction (OER). Across 15 noble-metal alloy and multicomponent oxide materials libraries, the different embedding choices occupy distinct regions of the trade-off between candidate reduction and robustness: element-wise, MatSciBERT often retains large fractions of the library, Qwen and the composition-prompt variants typically lie in an intermediate regime, and the lightweight Word2Vec baseline frequently achieves the largest reductions while staying close to the best measured performance. Comparisons between element-wise and composition-prompt transformers show that encoding full composition strings can improve robustness in specific systems but is not uniformly superior. Our results indicate that screening performance is governed jointly by the embedding model and by how stoichiometry is represented, and that simple text-based embeddings can serve as part of an effective filtering strategy that narrows experimental search spaces while keeping compositional diversity for follow-up study.

AUTHOR CONTRIBUTIONS

Lei Zhang: Conceptualization, Methodology, Software, Validation, Formal analysis, Investigation, Data Curation, Writing - Original Draft, Visualization, Experimentation, Funding acquisition.

Markus Stricker: Conceptualization, Resources, Supervision, Writing - Review & Editing, Funding acquisition.

ACKNOWLEDGMENTS

Both authors acknowledge inspiring discussions with Maribel Acosta (TUM) and Alfred Ludwig (RUB). We also acknowledge funding by the Deutsche Forschungsgemeinschaft (DFG, German Research Foundation) under CRC 1625, project number 506711657 (subprojects INF, A05). Lei Zhang acknowledges funding by the DFG through TRR 247, project number 388390466 (subproject INF).

DATA AND CODE AVAILABILITY

The code required to reproduce the results of this study is publicly available at https://github.com/lab-mids/w2v_transformers_materials_embeddings#. The full experimental datasets used in this study are publicly available via Zenodo: ORR dataset at <https://doi.org/10.5281/zenodo.13992986>, HER dataset at <https://doi.org/10.5281/zenodo.14959252>, and OER dataset (Ni-Pd-Pt-Ru) at <https://doi.org/10.5281/zenodo.14891704>. The Cr-Mn-Fe-Co-Ni-O series dataset is available from the corresponding publication at <https://doi.org/10.1021/acs.chemmater.2c01455>. Additional material-system files will be released publicly in a subsequent update of the repository/Zenodo record.

REFERENCES

- ¹Tobias Löffler, Alfred Ludwig, Jan Rossmeisl, and Wolfgang Schuhmann. What makes high-entropy alloys exceptional electrocatalysts? *Angewandte Chemie - International Edition*, 60(52):26894 – 26903, 2021. All Open Access; Green Accepted Open Access; Green Open Access; Hybrid Gold Open Access.
- ²Alfred Ludwig. Discovery of new materials using combinatorial synthesis and high-throughput characterization of thin-film materials libraries combined with computational methods. *npj Computational Materials*, 5:70, 2019.
- ³Yonggang Yao, Zhenan Huang, Tangyuan Li, Hang Wang, Yifan Liu, H. S. Stein, Yimin Mao, Jinlong Gao, Miaolun Jiao, Qi Dong, Jiaqi Dai, Pengfei Xie, Hua Xie, Steven David Lacey, Ichiro Takeuchi, John Mathew Gregoire, Rongzhong Jiang, Chao Wang, André D. Taylor, Reza Shahbazian-Yassar, and Liangbing Hu. High-throughput, combinatorial synthesis of multimetallic nanoclusters. *Proceedings of the National Academy of Sciences of the United States of America*, 117(12):6316 – 6322, 2020. All Open Access; Green Accepted Open Access; Green Open Access; Hybrid Gold Open Access.
- ⁴Sung Hyeon Baeck, Thomas Francisco Jaramillo, Christof Brändli, and Eric W. McFarland. Combinatorial electrochemical synthesis and characterization of tungsten-based mixed-metal oxides. *Journal of Combinatorial Chemistry*, 4(6):563 – 568, 2002.
- ⁵Neeraj Kumar Pandit, Diptendu Roy, Shyama Charan Mandal, and Biswarup Pathak. Rational designing of bimetallic/trimetallic hydrogen evolution reaction catalysts using supervised machine learning. *Journal of Physical Chemistry Letters*, 13(32):7583 – 7593, 2022.
- ⁶Xinghui Liu, Lirong Zheng, Chenxu Han, Hongxiang Zong, Guang Yang, Shiru Lin, Ashwani Kumar, Amol R. Jadhav, Ngoc Quang Tran, Yosep Hwang, Jinsun Lee, Suresh Vasimalla, Zhongfang Chen, Seong-gon Kim, and Hyoyoung Lee. Identifying the activity origin of a cobalt single-atom catalyst for hydrogen evolution using supervised learning. *Advanced Functional Materials*, 31(18), 2021.
- ⁷Vahe Tshitoyan, John M. Dagdelen, Leigh Weston, Alexander Dunn, Ziqin Rong, Olga Kononova, Kristin A. Persson, Gerbrand Ceder, and Anubhav Jain. Unsupervised word embeddings capture latent knowledge from materials science literature. *Nature*, 571(7763):95 – 98, 2019. All Open Access; Green Accepted Open Access; Green Open Access.
- ⁸Rubayat Mahbub, Kevin J. Huang, Zach Jensen, Zachary David Hood, Jennifer L.M. Rupp, and Elsa A. Olivetti. Text mining for processing conditions of solid-state battery electrolyte. *Electrochemistry Communications*, 121, 2020. All Open Access; Gold Open Access; Green Accepted Open Access; Green Open Access.
- ⁹Xiaowen Sun, Rafael B. Araujo, Egon Campos Dos Santos, Yuanhua Sang, Hong Liu, and Xiaowen Yu. Advancing electrocatalytic reactions through mapping key intermediates to active sites via descriptors. *Chemical Society Reviews*, 53(14):7392 – 7425, 2024.
- ¹⁰Dawei Chen, Chungli Dong, Yuqin Zou, Dong Su, Yucheng Huang, Li Tao, Shuo Dou, Shao Hua Shen, and Shuangyin Wang. In situ evolution of highly dispersed amorphous coo clusters for oxygen evolution reaction. *Nanoscale*, 9(33):11969 – 11975, 2017. All Open Access; Green Accepted Open Access; Green Open Access.
- ¹¹Mo Qiao, Cheng Tang, Guanjie He, Kaipei Qiu, Russell Binions, Ivan P. Parkin, Qiang Zhang, Zheng Xiao Guo, and Maria Magdalena Titirici. Graphene/nitrogen-doped porous carbon sandwiches for the metal-free oxygen reduction reaction: Conductivity: versus active sites. *Journal of Materials Chemistry A*, 4(32):12658 – 12666, 2016.
- ¹²Lei Zhang and Markus Stricker. Electrocatalyst discovery through text mining and multi-objective optimization, 2025.
- ¹³Jiaxing Qu, Yuxuan Richard Xie, Kamil M. Ciesielski, Claire E. Porter, Eric S. Toberer, and Elif Ertekin. Leveraging language representation for materials exploration and discovery. *npj Computational Materials*, 10(1), 2024. All Open Access; Gold Open Access.
- ¹⁴Ge Lei, Ronan Docherty, and Samuel J. Cooper. Materials science in the era of large language models: a perspective. *Digital Discovery*, 3(7):1257 – 1272, 2024. All Open Access; Gold Open Access.
- ¹⁵Hyunsoo Park, Anthony Onwuli, Keith T. Butler, and Aron Walsh. Mapping inorganic crystal chemical space. *Faraday Discussions*, 256:601 – 613, 2024. Cited by: 12.
- ¹⁶Siyu Liu, Tongqi Wen, A. S.L.Subrahmanyam Pattamatta, and David J. Srolovitz. A prompt-engineered large language model, deep learning workflow for materials classification. *Materials Today*, 80:240 – 249, 2024.
- ¹⁷Omer Levy and Yoav Goldberg. Neural word embedding as implicit matrix factorization. In *Advances in Neural Information Processing Systems (NeurIPS)*, 2014.
- ¹⁸Jacob Devlin, Ming-Wei Chang, Kenton Lee, and Kristina Toutanova. BERT: Pre-training of deep bidirectional transformers for language understanding. In Jill Burstein, Christy Doran, and Tamar Solorio, editors, *Proceedings of the 2019 Conference of the North American Chapter of the Association for Computational Linguistics: Human Language Technologies, Volume 1 (Long and Short Papers)*, pages 4171–4186, Minneapolis, Minnesota, June 2019. Association for Computational Linguistics.
- ¹⁹Tomas Mikolov, Kai Chen, Greg Corrado, Jeffrey Dean, L Sutskever, and Geoffrey Zweig. word2vec. URL <https://code.google.com/p/word2vec/>, 22:795, 2013.

- ²⁰Tomas Mikolov, Kai Chen, Greg Corrado, and Jeffrey Dean. Efficient estimation of word representations in vector space. In *Proceedings of the International Conference on Learning Representations (ICLR), Workshop Track*, 2013.
- ²¹Yoav Goldberg and Omer Levy. word2vec explained: deriving mikolov et al.’s negative-sampling word-embedding method. arXiv:1402.3722, 2014.
- ²²Tanishq Gupta, Mohd Zaki, N. M. Anoop Krishnan, and null Mausam. Matscibert: A materials domain language model for text mining and information extraction. *npj Computational Materials*, 8(1), 2022. All Open Access; Gold Open Access.
- ²³Jinze Bai, Shuai Bai, Yunfei Chu, Zeyu Cui, Kai Dang, Xiaodong Deng, Yang Fan, Wenbin Ge, Yu Han, Fei Huang, Binyuan Hui, Luo Ji, Mei Li, Junyang Lin, Runji Lin, Dayiheng Liu, Gao Liu, Chengqiang Lu, Keming Lu, Jianxin Ma, Rui Men, Xingzhang Ren, Xuancheng Ren, Chuanqi Tan, Sinan Tan, Jianhong Tu, Peng Wang, Shijie Wang, Wei Wang, Shengguang Wu, Benfeng Xu, Jin Xu, An Yang, Hao Yang, Jian Yang, Shusheng Yang, Yang Yao, Bowen Yu, Hongyi Yuan, Zheng Yuan, Jianwei Zhang, Xingxuan Zhang, Yichang Zhang, Zhenru Zhang, Chang Zhou, Jingren Zhou, Xiaohuan Zhou, and Tianhang Zhu. Qwen technical report. *arXiv preprint arXiv:2309.16609*, 2023.
- ²⁴Lei Zhang and Markus Stricker. Matnexus: A comprehensive text mining and analysis suite for materials discovery. *SoftwareX*, 26:101654, 2024.
- ²⁵Anna Rogers, Olga Kovaleva, and Anna Rumshisky. A primer in bertology: What we know about how bert works. *Transactions of the Association for Computational Linguistics*, 8:842 – 866, 2020.
- ²⁶Alexandre Strube. Helmholtz Blablador and the LLM models’ ecosystem, Apr 2024.
- ²⁷Lucas Foppa, Luca M. Ghiringhelli, Frank Girgsdies, Maïke Hashagen, Pierre Kube, Michael Hävecker, Spencer J. Carey, Andrey Tarasov, Peter Kraus, Frank Rosowski, Robert Schlögl, Annette Trunschke, and Matthias Scheffler. Materials genes of heterogeneous catalysis from clean experiments and artificial intelligence. *MRS Bulletin*, 46(11):1016 – 1026, 2021.
- ²⁸Vilfredo Pareto. *Cours d’Économie Politique professé à l’Université de Lausanne*, volume I–II. F. Rouge, Lausanne, Switzerland, 1896–1897.